Organic & Biomolecular Chemistry

Cite this: *Org. Biomol. Chem.*, 2011, **9**, 423

www.rsc.org/obc

PAPER

Effect of Sr^{2+} association on the tautomerization processes of uracil and its dithio- and diseleno-derivatives†

Ane Eizaguirre,[a] Otilia Mó,[a] Manuel Yáñez*[a] and Russell J. Boyd[b]

Received 20th June 2010, Accepted 17th September 2010
DOI: 10.1039/c0ob00292e

The structures and relative stabilities of the complexes formed by uracil and its thio- and seleno-derivatives with the Sr^{2+} cation, in the gas phase, have been analyzed by means of G96LYP density functional theory (DFT) calculations. The attachment of the Sr^{2+} cation to the heteroatom at position 4 is preferred systematically. Although the enolic forms of uracil and its derivatives should not be observed in the gas phase, the corresponding Sr^{2+} complexes are the most stable. The enhanced stability of these tautomers is two-fold, on the one hand Sr^{2+} interacts with two basic sites simultaneously, and on the other hand an aromatization of the six-membered ring takes place upon Sr^{2+} association. Sr^{2+} attachment also has a clear catalytic effect in the tautomerization processes involving uracil and its derivatives. This catalytic effect increases when oxygen is replaced by sulfur or selenium. The Sr^{2+} binding energy with uracil and its derivatives is bigger than the tautomerization barriers connecting the dioxo forms with the corresponding enolic tautomers. Consequently, when associated with Sr^{2+}, all tautomers are energetically accessible and should all be observed in the gas phase.

Introduction

Tautomerization processes of the nucleobases appear to be crucial in order to explain the mutation occurring during DNA duplication.[1,2] These tautomerization processes favor a non Watson and Crick base-pairing, giving rise to mutagenic processes.

The properties and reactivity of the nucleobases have been studied extensively during the last decade due to their important biological functions in living systems, including genetic information storage, gene expression, and catalysis.[3–6] Also, nucleobase thio-derivatives have attracted much interest.[7–11] In particular, 2-thiouracil and 4-thiouracil, identified as a minor component of t-RNA, can be used as anticancer and antithyroid drugs.[12] On the other hand, the replacement of the oxygen on the nucleobases by sulfur[13,14] has provided insight into DNA duplex stability, recognition, and replication at the atomic level.[15,16] Recent studies on these sulfur modifications have revealed enhanced base-pairing selectivity[17] and replication efficiency and fidelity, especially with the 2-thiothymidine.[18] Since selenium is much larger than oxygen, the replacement of O by Se will provide an insight into base pairing selectivity. Recently, Se derivatives of DNA nucleobases have been synthesized, and their crystal structures, thermostabilities, and the impact of their incorporation into oligonucleotides have been studied.[19] In addition, specific pyrimidines in natural tRNAs have been derivatized by the incorporation of Se onto the nucleobases.[20]

In view of the increasing interest in the thio- and seleno-derivatives of the nucleobases, much effort has been devoted to exploring the reactivity changes caused by replacing oxygen by sulfur and selenium in small biological systems. In the particular case of uracil and its thio- and seleno-derivatives, in order to rationalize the intrinsic reactivity, a great deal of attention has been devoted to the study of the tautomerization processes that these molecules can undergo.[11,21] These studies have found that dioxo, dithio and diseleno tautomers are the most stable forms, and the height of the barriers connecting them with the corresponding enolic forms are high enough to conclude that only the aforementioned forms may be observed experimentally in the gas phase under normal conditions.

The aim of this paper is to investigate the interaction of uracil and its derivatives with the Sr^{2+} cation and the effects that these interactions may have on the tautomerization of these systems, or on the relative stability of the different tautomers. It is well known that Sr^{2+} often mimics the behavior of Ca^{2+} in the human body, both having similar bone-seeking properties. Although in this media Sr is a trace metal, there is an increasing awareness of the biological role of Sr after the development of the drug strontium ranelate, which has been shown to reduce the incidence of fractures in osteoporotic patients.[22–24] With this work, we also aim to gain some insight into the reactivity of this cation with small biological systems. Although the interactions of strontium, calcium and copper ions with the DNA and RNA bases have been largely reported in the literature,[25–31] to the best of our knowledge there is no information available about the catalytic effect that these

[a]*Departamento de Química, Módulo 13. Universidad Autónoma de Madrid. Cantoblanco, Campus de Excelencia UAM-CSIC, 28049-Madrid, Spain*
[b]*Department of Chemistry, Dalhousie University, Halifax, Nova Scotia, B3H 4J3, Canada*

† Electronic supplementary information (ESI) available: Tables S1 and S2 and Fig. S1 and S2. See DOI: 10.1039/c0ob00292e

metals may have on the tautomerization processes studied in this work

Computational details

The geometries were optimized using density functional theory (DFT). For this purpose we have chosen the hybrid functional G96LYP,[32,33] as implemented in the Gaussian 03 suite of programs,[34] because in a previous assessment,[35] it has been shown to provide reliable results when dealing with Sr^{2+} interactions. We have used the basis sets proposed in ref. 26, namely 6-31+G(d,p) basis set expansion for C, O, N and H atoms, and an improved LAN2DZ[35] basis set for the Sr^{2+} cation (basis set A). Nevertheless, in order to ensure the reliability of the estimated stability of the different adducts, the final energy of each of the systems investigated was obtained in single-point calculations using a much larger and flexible 6-311+G (3df,2p) basis sets expansion for C, N, O, S, Se and H atoms, and an extended LAN2DZ (described in more detail in ref. 26) for Sr^{2+} cation (basis set B). Harmonic vibrational frequencies were computed at the same level used for geometry optimization in order to estimate the corresponding zero-point vibrational energy (ZPVE) corrections and to classify stationary points of the potential energy surface either as local minima or transition states (TS). Sr^{2+} binding energies were evaluated by subtracting from the energy of the most stable adduct, the energy of the neutral adduct and that of Sr^{2+}, after including the corresponding ZPVE corrections.

The bonding characteristics were analyzed primarily by using the Becke and Edgecombe electron localization function (ELF)[36] topological approach,[37] which provides useful information about the nature of the bonding, even in challenging cases in which other approaches fail to give an unambiguous bonding picture.[38] ELF has been originally conceived as a local measure of the Fermi hole curvature around a reference point. A Lorentz transform allows ELF to be confined in the [0,1] interval, where 1 corresponds to regions dominated by an opposite spin pair or by a single electron. In this way, the molecular space can be partitioned in basins so that the valence shell of a molecule can be described in terms of two types of basins: polysynaptic basins (generally disynaptic), with the partition of two (or more) atomic valence shells and monosynaptic ones, which correspond to electron lone-pairs or core electrons. ELF calculations were carried out with the TopMod suite of programs.[39]

A second approach, the atoms in molecules (AIM) theory,[40,41] was also used in our bonding study. This theory is based on a topological analysis of the electron density, which permits the definition of a molecular graph as the ensemble of bond critical points (BCPs), stationary points in which the electron density is minimum only in the direction of the bond, and bond paths. In general, the electron density, as well as the energy density calculated at the BCPs, gives useful information on the strength and nature of the bond. For this purpose the AIMPAC series of programs was employed.[42] These analyses were complemented with natural bond orbital (NBO) and natural resonance theory (NRT) calculations.[43] The former permits the bonding to be described in terms of localized hybrids and lone-pairs, and the second provides the weight of the different resonant structures that contribute to the stability of a given system. In both cases the Sadlej basis set was used due to the reliability of all electron basis sets when dealing with electron density topological analysis. The Wiberg bond orders (BO) were also evaluated in the framework of the former approach. These calculations have been carried out with the NBO-5G series of programs.[44]

As we shall discuss in forthcoming sections, aromaticity plays a non-negligible role on the stability of some uracil-Sr^{2+} complexes. In order to analyze this property we will use two different indexes, a magnetic one, the nucleus independent chemical shift (NICS),[45] and a structural one, the harmonic oscillator model of aromaticity (HOMA)[46] index. The NICS is defined as the negative absolute magnetic shielding computed in the centre of the ring (NICS(0)), or 1 Å above the ring centre (NICS(1)).[47] Rings with highly negative NICS values are aromatic whereas those with positive values are usually anti-aromatic. Since the average isotropic values of NICS can be unreliable for some systems,[45,48] we will analyze instead the values of $NICS_{zz}$, which corresponds to the zz-component of the shielding tensor, which has been shown to be a better aromaticity index than isotropic NICS.

The HOMA index is defined as

$$\mathrm{HOMA} = 1 - \frac{\alpha}{n}\sum\left[R_{\mathrm{opt}} - R_{\mathrm{i}}\right]^2 \qquad (2)$$

where R_{opt} is an empirically estimated optimal bond length assumed to be obtained when full delocalization of π-electrons occurs and used as a suitable reference value. R_{i} stands for the bond lengths in the system under investigation, n is the number of bonds considered and α is an empirical constant chosen so that HOMA is zero for the hypothetical Kekulé structures of an aromatic system, and 1 when all bonds are equal to the optimal value R_{opt}. For CC bonds $\alpha = 257.7$ and $R_{\mathrm{opt}} = 1.388$.

Results and discussion

Uracil and its thio- and seleno-derivatives, and the most stable structures of corresponding tautomeric forms in the presence of the Sr^{2+} cation, are represented in Scheme 1. The atom numbering shown in structure **a** will be used throughout. Heteroatoms bonded to C4 and C2 are designated as X and Y, respectively. The conformers of each tautomer are named by adding **a** or **b** to the number identifying the tautomer. The relative energies of these compounds are shown in Table 1, whereas their total energies and ZPVE corrections are given in Table S1, ESI.† The optimized geometry of the most stable tautomer for each compound is presented in Table S2, ESI.†

Geometries, relative stabilities and bonding

As observed previously for Ca^{2+} and Li^{+},[49,50] the C═O–Sr^{2+} angles of uracil complexes are always equal to or very close to 180°. Conversely, for dithio-and diseleno-uracil complexes, the S–Sr^{2+} and the Se–Sr^{2+} bonds do not lie in the plane of the molecule, but in a plane perpendicular to it, similar to what was previously reported for Ca^{2+} complexes.[50,51] A suitable explanation of these features was provided assuming that the primary interaction of these bonds is electrostatic.[49] When the basic site is a carbonyl oxygen, the metal dication polarizes both oxygen lone-pairs simultaneously, and consequently it nests between them. When the basic site is a sulfur or selenium atom, whose lone pairs are much more voluminous, the metal dication is unable to polarize both lone pairs at the same time, and therefore it interacts preferentially with one of them.

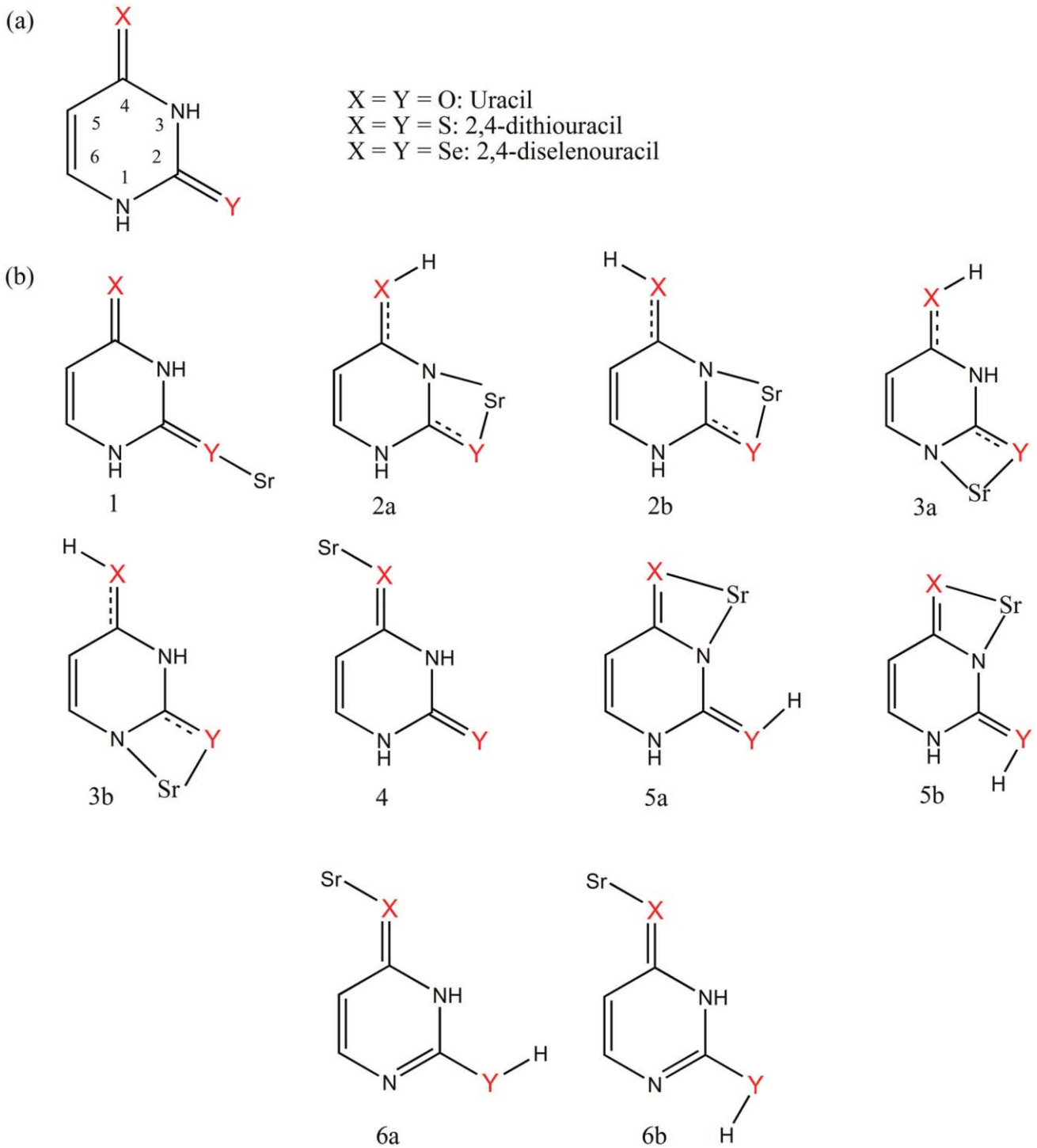

Scheme 1 Schematic representation of: a) uracil and its thio- and seleno-derivatives; b) different tautomeric forms of uracil-Sr^{2+}, 2,4-dithiouracil-Sr^{2+} and 2,4-diselenouracil-Sr^{2+} complexes.

Whereas for uracil-Ca^{2+}, a π-type complex exists as a local minimum,[52] and in the case of uracil-Sr^{2+} and 2,4-dithiouracil-Sr^{2+}, this π-type complex exists as a transition state structure. This transition state connects adduct **1** with adduct **4**. However, no π-type stationary point for the 2,4-diselenouracil-Sr^{2+}complex has been found, as it collapses to form either **1** or **4**. The energy, ZPVE and optimized structure of the aforementioned π-type transition state complexes are available in Table S1 and Table S2, respectively, ESI.† It is also worth noting that any attempt to attach the metal dication to the olefinic bond failed because these structures were not stationary points on the potential energy surface.

Only in the case of 2,4 dithio- and 2,4-diseleno-uracil, adduct **7** (See Fig. 1) is a local minimum on the potential energy surface.[50,51] The enhanced stability of structure **7** when dealing with thio- or

Table 1 Relative energies (kJ mol^{-1}) of the different tautomeric forms of uracil and its thio- and seleno-derivatives in the presence of the Sr^{2+} cation

Tautomer	Uracil	2,4-dithiouracil	2,4-diselenouracil
1	74	120	129
2a	21	17	16
2b	0	0	5
3a	30	3	0[a]
3b	14	1	0[a]
4	34	94	95
5a	27	—[b]	—[b]
5b	26	19	21
6a	105	110	105
6b	64	100	103
7	—[b]	114	97

[a] The energy difference between tautomers **3a** and **3b** decreases as O > S > Se and for the Se derivatives both forms are practically degenerate at the G96LYP/B//G96LYP/A. This is likely to be due to a repulsive interaction between the H attached to the heteroatom X and the near NH group, which decreases as the electronegativity of X decreases. [b] These structures are not stationary points on the potential energy surface.

Table 2 Sr^{2+} binding energies (kJ mol^{-1}) of uracil and its thio- and seleno-derivatives at basic sites X and Y

Compound	X	Y
Uracil	371.9	331.9
2,4-dithiouracil	324.3	298.6
2,4-diselenouracil	334.9	301.1

Table 3 Wiberg bond orders for uracil and **1** and **4** uracil-Sr^{2+} complexes

Bond	Uracil	**1**	**4**
N1–C2	1.05	1.22	1.03
C2–N3	1.10	1.31	1.00
N3–C4	1.03	0.90	1.22
C4–C5	1.10	1.11	1.28
C5–C6	1.68	1.72	1.50
C6–N1	1.15	1.08	1.29

seleno-derivatives has been well documented in ref. 43. On the one hand, sulfur and selenium are less electronegative than oxygen and consequently, when oxygen is replaced by its heavier homologues, an accumulation of electron density on the N3 lone pairs occurs. On the other hand, sulfur and selenium are much more polarizable than oxygen and consequently, adduct **7** is stabilized through the enhanced polarization of these two heteroatoms. This is clearly mirrored in the existence of the disynaptic basins V(Sr,S) of the corresponding ELF (See Fig. 2) and by the presence of the Sr–S BCPs of the AIM molecular graph (See Fig. 1). The greater polarizability of the selenium atom relative to the sulfur atom explains why the 2,4-diselenouracil-Sr^{2+} structure **7** is more stable than the corresponding 2,4-dithiouracil-Sr^{2+} complex.

As was found previously for the Ca^{2+} dication,[50,51] Sr^{2+} shows a clear preference to bind to the heteroatom at position 4 (X) with respect to the heteroatom at position 2 (Y). The enhanced basicity of the heteroatom X with respect to heteroatom Y has been attributed to the contribution of zwitterionic mesomeric forms which accumulate negative charge in this position.[7,53–55] However, as has been already pointed out in a previous work,[50] similar mesomeric forms accumulating negative charge at Y also contribute to the stability of the neutral compound, so this single factor cannot explain the preference of uracil and its thio- and seleno-derivatives to undergo electrophilic attack at X. There is, however, another effect which explains the enhanced basicity of heteroatom X with respect to Y, this being the considerably larger electron delocalization induced within the uracil ring when the cation is attached to X.[50] This explanation is consistent with the ELF plots shown in Fig. 2 for uracil and uracil-Sr^{2+} complexes **1** and **4**. The populations of the basins associated with the C5–C6, C5–C4, C4–N3 and C6–N1 bonds changes very little on going from uracil to complex **1**, showing that the strong electron localization observed in the neutral compound, is practically unaltered by Sr^{2+} attachment to Y. Conversely, on going from neutral uracil to complex **4**, where the metal is attached to X, a significant electron density delocalization is observed from C5–C6 towards the C5–C4, C4–N3 and C6–N1 basins (See Fig. 2). This electron delocalization, which contributes to the stabilization of the molecular cation, is actually mirrored in a certain equalization of the bond distances within the ring (See Figure S1, ESI†), the electron densities at the corresponding BCPs (see Fig. 1), and the Wiberg bond orders (see Table 3). In neutral uracil, C5–C6 has a significant double bond character, whereas the remaining bonds within the ring are essentially single bonds. In the case of complex **4**, the charge polarization produced by Sr^{2+} attachment diminishes the double bond character of C5–C6, while increasing that of the C5–C4, C6–C1 and C3–C4 bonds. Conversely, in complex **1**, only C2–N3 and C2–N1 increase their double bond character, ratifying the strong electron density localization in this system. Similar trends are also observed for 2,4-dithio- and 2,4-diselenouracil.

The greater Sr^{2+} binding energy for uracil with respect to 2,4-dithiouracil and 2,4-diselenouracil, reveals a higher preference of Sr^{2+} to attach to oxygen rather than to sulfur or selenium (see Table 2). This is likely to be a direct consequence of the electrostatic nature of the Sr–O, Sr–S and Sr–Se interactions, as reflected in the small value of the electron density at the corresponding BCPs (See Fig. 1), and in the positive value of its Laplacian. Since O is much smaller than S and Se, the distance between the basic site and the metal dication is much shorter, enhancing the electrostatic interaction which is not compensated by the larger polarizability of S and Se. An influence of the interaction of the ion with the bond dipole associated with the C═X (X═O, S, Se) bond cannot be discarded. The second highest Sr^{2+} binding energy is for 2,4-diselenouracil, which confirms the greater polarizability of selenium relative to the sulfur atom. The same trend was found in the case of the Ca^{2+} cation.[50,51]

Also, NBO analysis consistently does not show the existence of any covalent bond between Sr and the base. When the metal dication is attached to the C═X (X═O, S, Se) bonds, the electron density at the corresponding C = X BCPs decreases significantly, as well as the population of the corresponding basins, as shown in Fig. 1 and 2, respectively. This effect, which actually diminishes on going from oxygen to selenium, reflects the heteroatom's polarizability increase on going from oxygen to selenium. Also, the natural charge of the metal diminishes on going from uracil-Sr^{2+} to 2,4-diselenouracil-Sr^{2+}, reflecting the stronger polarization undergone by the heteroatom in the presence of the Sr^{2+} cation when oxygen is substituted by sulfur and selenium atoms.

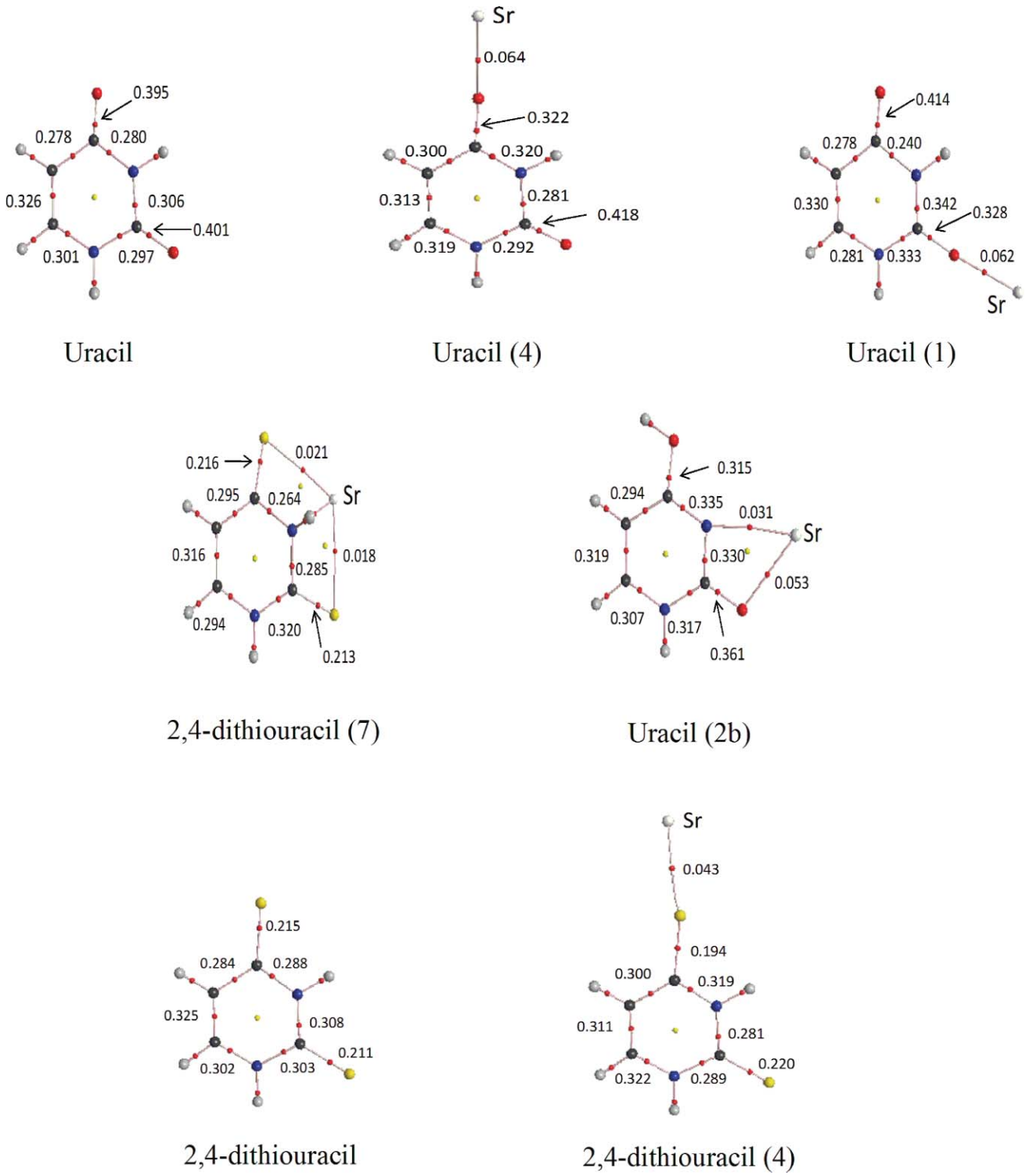

Fig. 1 Molecular graphs of neutral uracil, neutral 2,4-dithiouracil, **1**, **4** and **2b** uracil-Sr^{2+} complexes and **4** and **7** 2,4-dithiouracil-Sr^{2+} complexes. Electron densities at BCPs are in a.u.

Tatomerization processes. Catalytic effect of Sr^{2+} association

Dioxo, dithio and diseleno are the only tautomeric forms of uracil and its thio- and seleno-derivatives present in the gas phase under normal conditions. Therefore, only adducts **1** and **4** can be formed by direct association of the Sr^{2+} cation at the available basic sites. However, considering all the tautomers represented in Scheme 1, the aforementioned adducts are the least stable in the gas phase. As pointed out in previous work,[31,50,51] the presence of the metal dication completely alters the stability order, the most stable isomers being **2a**, **2b**, **3a**, **3b** and **5b** enolic forms. The enhanced stability of these tautomeric forms with respect to the structures **1**

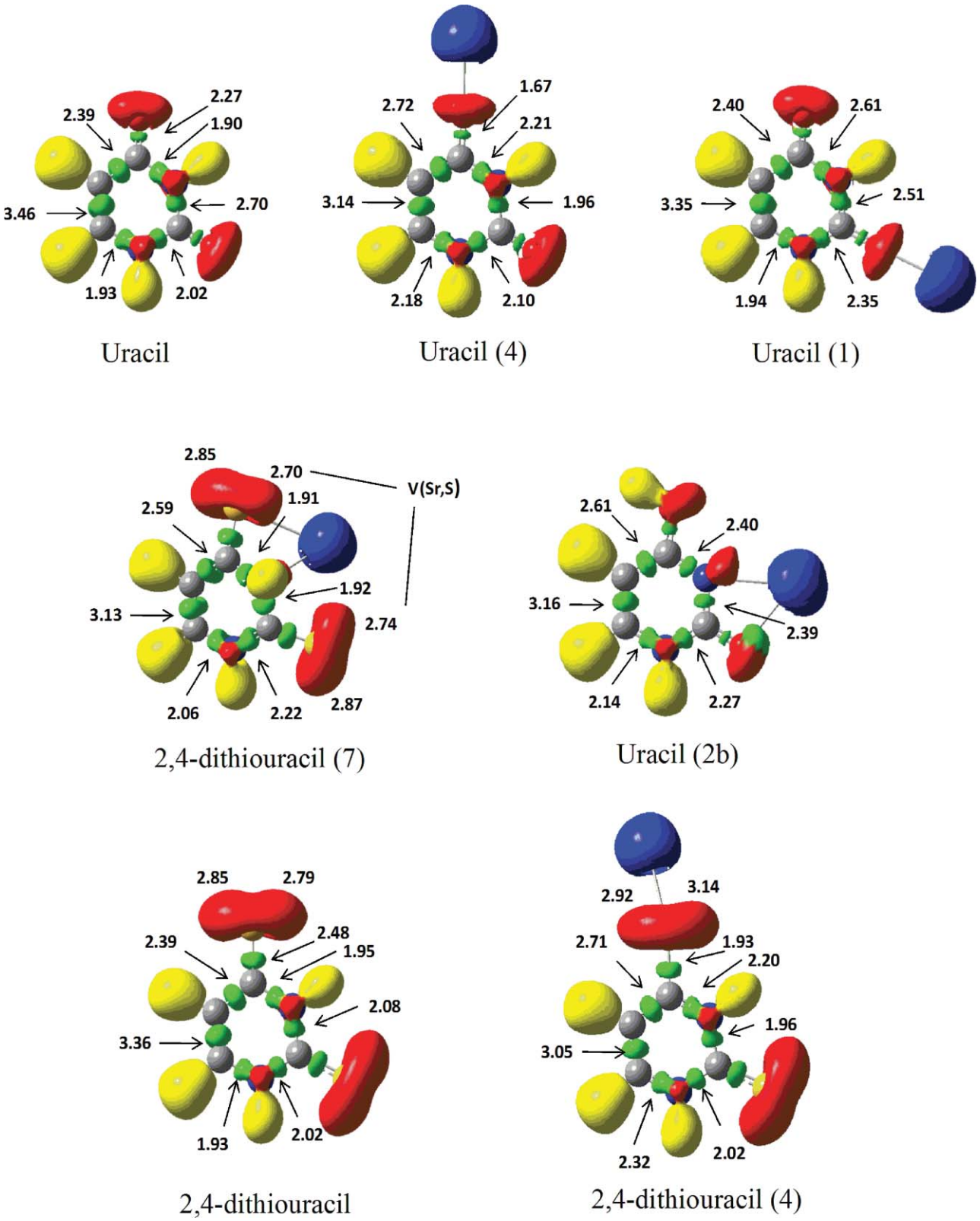

Fig. 2 Three dimensional representation of ELF isosurface with ELF = 0.80 for neutral uracil, neutral 2,4-dithiouracil, **1**, **4** and **2b** uracil-Sr^{2+} complexes and **4** and **7** 2,4-dithiouracil-Sr^{2+} complexes. Yellow lobes correspond to V(N,H) and V(C,H) basins, red lobes correspond to V(N), V(O) and V(S) basins associated with N, O and S lone-pairs, respectively. Green lobes correspond to V(C,C), V(C,N), V(C,O) and V(C,S). Blue lobes correspond to the Sr metal core. The populations of the different basins are also indicated.

Table 4 $NICS_{zz}(1)$ (in ppm) and HOMA for neutral uracil and 2,4-dithiouracil and their more stable complexes with Sr^{2+}

	Uracil	Uracil-Sr^{2+} (**2b**)	2,4-dithiouracil	2,4-dithiouracil-Sr^{2+} (**2b**)
NICSzz (1)	–1.8	–9.3	3.705	–4.457
HOMA	0.399	0.838	0.600	0.836

and **4** can be attributed to two factors.[50] The formation of the enolic form by 1,3H shifts from one of the NH groups towards X or Y heteroatom triggers the aromatization of the six-membered ring.

This aromatization is actually reflected in the equalization of the bond distances and in the BCP densities of the bonds within the ring on going from adduct **1** to complex **2b** (See Fig. 1), as well as in the values of the $NICS_{zz}$ and the HOMA (See Table 4). It is apparent that the $NICS_{zz}$ becomes significantly more negative on going from neutral uracil and 2,4-ditihiouracil to the most stable Sr^{2+} complexes, **2b**. Also the HOMA value is much closer to unity in the Sr^{2+} complexes than in the neutral compounds.

As found previously for thymine-M^{2+} (M = Ni, Cu, Zn) complexes,[56] the aromatization of the six-membered ring contributes a lot to the stabilization of the enolic form. On the other hand, and more importantly, the enolic structure facilitates the interaction of the metal dication with two basic sites simultaneously, an N-pyridine-like nitrogen and the X or Y heteroatom. This effect increases the stability of **2a**, **2b**, **3a**, **3b** and **5b** complexes. Consistently, the enolic forms, **6a** and **6b**, in which there is no possibility for the metal to polarize two basic sites simultaneously, are the least stable structures. In the case of uracil, the most stable complex corresponds to **2b**, in which Sr^{2+} simultaneously interacts with Y and N3 basic sites, whereas in the case of 2,4-dithiouracil complexes **2b** and **3b**, in which the metal interacts with Y and N1 atoms simultaneously, are practically degenerate. For 2,4-diselenouracil, the latter form is found to be 5 kJ mol^{-1} lower in energy than **2b**.

In view of the enhanced stability of the enolic forms with respect to structures **1** and **4**, we also studied the tautomerization processes required to connect adducts **1** and **4** with complexes **2** and **5**. Hence, in Fig. 3a–c the energy profiles associated with the **1** → **2**, **1** → **4** and **4** → **5** isomerization processes are shown. Note that, as mentioned before, for 2,4-diselenouracil, the global minimum is the **3b** enolic form, which is not included in Fig. 3 for the sake of consistency. Nevertheless, the corresponding isomerization process connecting **1** and **3b** is shown in Fig. S2, ESI.† The most significant finding is that all activation barriers lie below the entrance channel. This means that the direct association of Sr^{2+} with the neutral forms, should give them enough internal energy to overpass the barriers connecting the keto with the corresponding enolic forms. Consequently, all of the tautomeric forms should be energetically accessible upon Sr^{2+} attachment and therefore in the presence of this cation, all tautomeric forms might be observed in the gas phase. Another important feature is that the activation barriers involved in these tautomerization processes are much lower than those calculated for the isolated neutral compounds.[21,53] Similar findings have been reported for other metal ions such as Ca^{2+} and Cu^{+}.[50,51,57] In Table 5, the catalytic effect of the aforementioned metals, given by the decrease (%) in the barrier height upon metal cation association, has been summarized. It should be mentioned that, as shown in Fig. 3, when these barriers are measured in terms of free energies, the changes are very small and the observed catalytic effect is practically equal to that estimated using energies instead of free energies.

Table 5 Catalytic effects of the Sr^{2+}, Ca^{2+} and Cu^{+} cations in the tautomerization processes involving uracil, 2,4-dithiouracil and 2,4-diselenouracil

	Uracil	2,4-dithiouracil	2,4-diselenouracil
Sr^{2+}			
1→2	17%	40%	50%
4→5	22%	34%	35%
Ca^{2+}			
1→2	25%	37%	41%
4→5	20%	35%	35%
Cu^{+}			
1→2	20%	39%	31%
4→5	19%	32%	29%

In the case of the Ca^{2+} and Sr^{2+} cations, the catalytic effect of the metal increases as uracil < 2,4-dithiouracil < 2,4-diselenouracil. However in the case of the Cu^{+} cation, the largest catalytic effect is with 2,4-dithiouracil, and the second with 2,4-diselenouracil.

Conclusions

From our theoretical survey of the interaction between uracil and its thio- and seleno-derivatives with the Sr^{2+} cation in the gas phase, we can conclude that:

• The basicity of heteroatom X is systematically larger than that of heteroatom Y. This effect is due to the greater electron delocalization induced within the ring when the metal is attached to heteroatom X.

• Sr^{2+} presents a greater affinity for oxygen than for sulfur and selenium, likely due to the electrostatic nature of the interaction and to the much shorter Sr–O distances.

• In the case of uracil, the most stable complex corresponds to structure **2b**, whereas in the case of 2,4-dithiouracil and 2,4-diselenouracil, structures **2b** and **3b** are practically degenerate. Two factors are responsible for the enhanced stability of these enolic forms. On the one hand, in these structures the simultaneous interaction of the Sr^{2+} cation with two basic sites (N1 or N3 and X or Y heteroatom) is facilitated. On the other hand, a greater aromatization of the six-membered ring takes place in these structures.

• Sr^{2+} binding energies with uracil and its derivatives are greater than the activation barriers which connect diketo-like with enolic-like complexes. Consequently, upon Sr^{2+} interaction all tautomers should be energetically accessible, and all of them should be observed in the gas phase.

• Sr^{2+} and Ca^{2+} show almost identical catalytic effects on the tautomerization processes involving uracil-Sr^{2+}, 2,4-dithiouracil-Sr^{2+} and 2,4-diselenouracil-Sr^{2+} complexes. In both cases, the catalytic effect increases on going from uracil to 2,4-diselenouracil. However, for Cu^{+} the largest catalytic effect is observed for the 2,4-dithiouracil complexes.

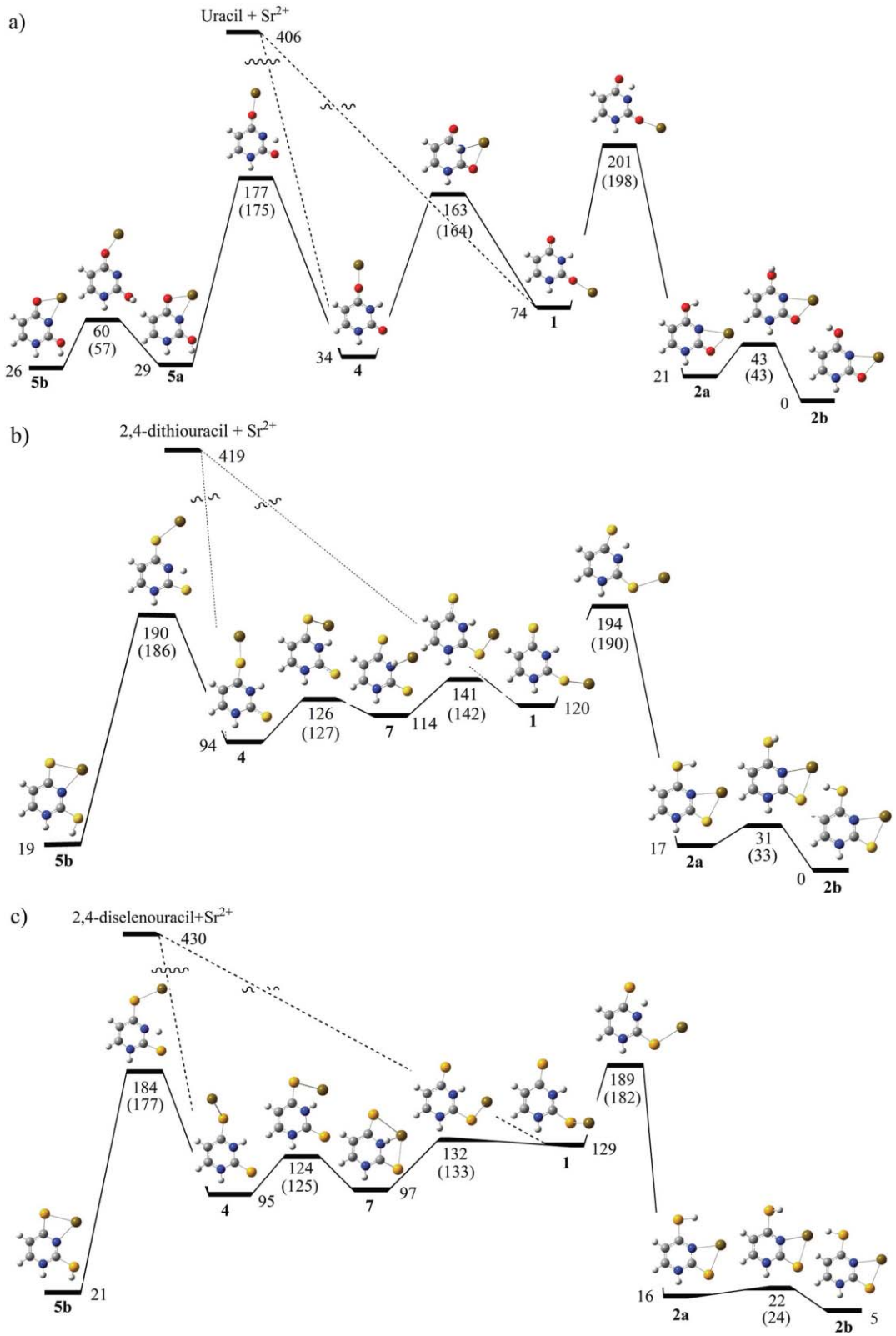

Fig. 3 Energy profiles for the isomerization process of: a) uracil-Sr^{2+} adducts; b) 2,4-dithiouracil-Sr^{2+} adducts; c) 2,4-diselenouracil-Sr^{2+} adducts. Relative energies are in kJ mol^{-1}. For the barriers, the values within parentheses were obtained using free energies.

Acknowledgements

This work has been partially supported by the DGI Project No. CTQ2009-13129-C01, by the Project MADRISOLAR2, Ref.: S2009PPQ/1533 of the Comunidad Autónoma de Madrid, by Consolider on Molecular Nanoscience CSD2007-00010, and by the COST Action CM0702. The financial support of the Natural Sciences and Engineering Research Council of Canada (to RJB) is gratefully acknowledged. A generous allocation of computing time at the CCC of the UAM is also acknowledged.

References

1 Gottscha. Em, E. Kopp and A. G. Lezius, *Eur. J. Biochem.*, 1971, **24**, 168.
2 W. Saenger and D. Suck, *Eur. J. Biochem.*, 1973, **32**, 473–478.
3 G. Storz, *Science*, 2002, **296**, 1260–1263.
4 S. R. Eddy, *Nat. Rev. Genet.*, 2001, **2**, 919–929.
5 M. R. Latham, D. J. Brown, S. A. McCallum and A. Pardi, *ChemBioChem*, 2005, **6**, 1492–1505.
6 K. E. Blount and O. C. Uhlenbeck, *Annu. Rev. Biophys. Biomol. Struct.*, 2005, **34**, 415–440.
7 A. R. Katritzky, G. Baykut, S. Rachwal, M. Szafran, K. C. Caster and J. Eyler, *J. Chem. Soc., Perkin Trans. 2*, 1989, 1499–1506.
8 A. R. Katritzky, M. Szafran and G. Pfisterguillouzo, *J. Chem. Soc., Perkin Trans. 2*, 1990, 871–876.
9 A. Les and L. Adamowicz, *J. Am. Chem. Soc.*, 1990, **112**, 1504–1509.
10 J. Leszczynski and K. Lammertsma, *J. Phys. Chem. A*, 1991, **95**, 3128–3132.
11 M. Lamsabhi, M. Alcami, O. Mó, W. Bouab, M. Esseffar, J. L. M. Abboud and M. Yáñez, *J. Phys. Chem. A*, 2000, **104**, 5122–5130.
12 W. Saeger, *Principles of the Nucleic Acids Structures*, Springer, New York, 1984.
13 M. Sprinzl, K. H. Scheit and F. Cramer, *Eur. J. Biochem.*, 1973, **34**, 306–310.
14 A. G. Lezius and K. H. Scheit, *Eur. J. Biochem.*, 1967, **3**, 85.
15 I. V. Kutyavin, R. L. Rhinehart, E. A. Lukhtanov, GornVv, R. B. Meyer and H. B. Gamper, *Biochemistry*, 1996, **35**, 11170–11176.
16 R. S. Coleman and E. A. Kesicki, *J. Am. Chem. Soc.*, 1994, **116**, 11636–11642.
17 A. M. Sismour and S. A. Benner, *Nucleic Acids Res.*, 2005, **33**, 5640–5646.
18 H. O. Sintim and E. T. Kool, *J. Am. Chem. Soc.*, 2006, **128**, 396–397.
19 J. Salon, J. Sheng, J. S. Jiang, G. X. Chen, J. Caton-Williams and Z. Huang, *J. Am. Chem. Soc.*, 2007, **129**, 4862.
20 C. S. Chen and T. C. Stadtman, *Proc. Natl. Acad. Sci. U. S. A.*, 1980, **77**, 1403–1407.
21 C. Trujillo, O. Mó and M. Yáñez, *Org. Biomol. Chem.*, 2007, **5**, 3092–3099.
22 P. J. Meunier, R. S. Lorenc, I. G. Smith, A. Roces-Varela, R. Passariello, O. Bonidan, H. P. Kruse, F. Raeman, R. Prince, R. De Chatel, P. Charles, J. Fechtenbaum, C. Roux and J. Y. Reginster, *Osteoporosis Int.*, 2002, **13**, P66.
23 P. J. Meunier, C. Roux, E. Seeman, S. Ortolani, J. E. Badurski, T. D. Spector, J. Cannata, A. Balogh, E. M. Lemmel, S. Pors-Nielsen, R. Rizzoli, H. K. Genant, J. Y. Reginster, J. Graham, K. W. Ng, R. Prince, J. Prins, J. Wark, J. P. Devogelaer, J. M. Kaufman, F. Raeman, J. P. Ziekenhuis, M. Walravens, H. Beck-Nielsen, P. Charles, O. H. Sorensen, J. P. Aquino, C. Benhamou, F. Blotman, O. Bonidan, P. Bourgeois, J. Dehais, P. Fardellone, A. Kahan, J. L. Kuntz, C. Marcelli, A. Prost, B. Vellas, G. Weryha, D. Felsenberg, J. Hensen, H. P. Kruse, W. Schmidt, J. Semler, G. Stucki, C. Phenekos, R. De Chatel, S. Adami, G. Bianchi, M. L. Brandi, D. Cucinotta, C. Fiore, C. Gennari, G. Isaia, G. Luisetto, R. Passariello, M. Passeri, G. Rovetta, L. Tessari, K. Hoszowski, R. S. Lorenc, A. Sawicki, A. Diez, J. B. Cannata, M. D. Curiel, A. Rapado, J. Gijon, A. Torrijos, J. M. Padrino, A. R. Varela, J. P. Bonjour, M. Clements, D. V. Doyle, P. Ryan, I. G. Smith and R. Smith, *N. Engl. J. Med.*, 2004, **350**, 459–468.
24 J. Y. Reginster, A. Sawicki, J. P. Devogelaer, J. M. Padrino, J. M. Kaufma, D. V. Doyle, P. Fardellone, J. Graham, D. Felsenberg, Z. Tulassay, O. H. Soren-Sen, G. Luisetto, R. Rizzoli, F. Blotman, C. Phenekos and P. J. Meunier, *Osteoporosis Int.*, 2002, **13**, O14.
25 T. Marino, D. Mazzuca, N. Russo, M. Toscano and A. Grand, *Int. J. Quantum Chem.*, 2010, **110**, 138–147.
26 T. Marino, M. Toscano, N. Russo and A. Grand, *Int. J. Quantum Chem.*, 2004, **98**, 347–354.
27 D. Mazzuca, N. Russo, M. Toscano and A. Grand, *J. Phys. Chem. B*, 2006, **110**, 8815–8824.
28 N. Russo, E. Sicilia, M. Toscano and A. Grand, *Int. J. Quantum Chem.*, 2002, **90**, 903–909.
29 N. Russo, M. Toscano and A. Grand, *J. Phys. Chem. B*, 2001, **105**, 4735–4741.
30 N. Russo, M. Toscano and A. Grand, *J. Am. Chem. Soc.*, 2001, **123**, 10272–10279.
31 N. Russo, M. Toscano and A. Grand, *J. Phys. Chem. A*, 2003, **107**, 11533–11538.
32 P. M. W. Gill, *Mol. Phys.*, 1996, **89**, 433–445.
33 C. T. Lee, W. T. Yang and R. G. Parr, *Phys. Rev. B: Condens. Matter*, 1988, **37**, 785–789.
34 M. J. Frisch, G. W. Trucks, H. B. Schlegel, G. E. Scuseria, M. A. Robb, J. R. Cheeseman, J. A. Montgomery, Jr., T. Vreven, K. N. Kudin, J. C. Burant, J. M. Millam, S. S. Iyengar, J. Tomasi, V. Barone, B. Mennucci, M. Cossi, G. Scalmani, N. Rega, G. A. Petersson, H. Nakatsuji, M. Hada, M. Ehara, K. Toyota, R. Fukuda, J. Hasegawa, M. Ishida, T. Nakajima, Y. Honda, O. Kitao, H. Nakai, M. Klene, X. Li, J. E. Knox, H. P. Hratchian, J. B. Cross, V. Bakken, C. Adamo, J. Jaramillo, R. Gomperts, R. E. Stratmann, O. Yazyev, A. J. Austin, R. Cammi, C. Pomelli, J. Ochterski, P. Y. Ayala, K. Morokuma, G. A. Voth, P. Salvador, J. J. Dannenberg, V. G. Zakrzewski, S. Dapprich, A. D. Daniels, M. C. Strain, O. Farkas, D. K. Malick, A. D. Rabuck, K. Raghavachari, J. B. Foresman, J. V. Ortiz, Q. Cui, A. G. Baboul, S. Clifford, J. Cioslowski, B. B. Stefanov, G. Liu, A. Liashenko, P. Piskorz, I. Komaromi, R. L. Martin, D. J. Fox, T. Keith, M. A. Al-Laham, C. Y. Peng, A. Nanayakkara, M. Challacombe, P. M. W. Gill, B. G. Johnson, W. Chen, M. W. Wong, C. Gonzalez and J. A. Pople, *GAUSSIAN 03 (Revision B.02)*, Gaussian, Inc., Wallingford, CT, 2004.
35 A. Eizaguirre, M. Yanez, J. Tortajada and J. Y. Salpin, *Chem. Phys. Lett.*, 2008, **464**, 240–244.
36 A. D. Becke and K. E. Edgecombe, *J. Chem. Phys.*, 1990, **92**, 5397–5403.
37 B. Silvi and A. Savin, *Nature*, 1994, **371**, 683–686.
38 O. Mó, M. Yáñez, A. M. Pendas, J. E. Del Bene, I. Alkorta and J. Elguero, *Phys. Chem. Chem. Phys.*, 2007, **9**, 3970–3977.
39 S. Noury, X. Krokidis, F. Fuster and B. Silvi, *Comput. Chem.*, 1999, **23**, 597–604.
40 R. F. W. Bader, *Atoms in Molecules. A Quantum theory*, Claredon Press, Oxford, 1990.
41 C. F. Matta and R. J. Boyd, *The Quantum Theory of Atoms in Molecules*, Wiley-VCH Verlag GmbH & Co., KGaA, Weinheim, 2007.
42 R. F. W. Bader and J. R. Cheeseman, AIMPAC Programs, 2000.
43 A. E. Reed, L. A. Curtiss and F. Weinhold, *Chem. Rev.*, 1988, **88**, 899–926.
44 E. D. Glendening, J. K. Badenhoop, A. E. Reed, J. E. Carpenter, J. A. Bohmann, C. M. Morales and F. Weinhold, *NBO 5. G.*, Theoretical Chemistry Institute, University of Wisconsin, Madison, WI, 2004.
45 P. V. Schleyer, C. Maerker, A. Dransfeld, H. J. Jiao and N. Hommes, *J. Am. Chem. Soc.*, 1996, **118**, 6317–6318.
46 T. M. Krygowski, *J. Chem. Inf. Comput. Sci.*, 1993, **33**, 70–78.
47 P. V. Schleyer, M. Manoharan, Z. X. Wang, B. Kiran, H. J. Jiao, R. Puchta and N. Hommes, *Org. Lett.*, 2001, **3**, 2465–2468.
48 Z. F. Chen, C. S. Wannere, C. Corminboeuf, R. Puchta and P. V. Schleyer, *Chem. Rev.*, 2005, **105**, 3842–3888.
49 M. Alcamí, O. Mó and M. Yáñez, *Molecular Electrostatic Potentials: Concepts and Applications*, Elsevier, Amsterdam, 1996.
50 C. Trujillo, A. M. Lamsabhi, O. Mó, M. Yáñez and J. Y. Salpin, *Org. Biomol. Chem.*, 2008, **6**, 3695–3702.
51 A. M. Lamsabhi, O. Mó, M. Yáñez and R. J. Boyd, *J. Chem. Theory Comput.*, 2008, **4**, 1002–1011.
52 W. L. Zhu, X. M. Luo, C. M. Puah, X. J. Tan, J. H. Shen, J. D. Gu, K. X. Chen and H. L. Jiang, *J. Phys. Chem. A*, 2004, **108**, 4008–4018.
53 M. Lamsabhi, M. Alcami, O. Mo, W. Bouab, M. Esseffar, J. L. M. Abboud and M. Yanez, *J. Phys. Chem. A*, 2000, **104**, 5122–5130.
54 M. T. Nguyen, A. K. Chandra and T. Zeegers-Huyskens, *J. Chem. Soc., Faraday Trans.*, 1998, **94**, 1277–1280.
55 M. A. Kurinovich, L. M. Phillips, S. Sharma and J. K. Lee, *Chem. Commun.*, 2002, 2354–2355.
56 E. Rincon, M. Yanez, A. Toro-Labbe and O. Mo, *Phys. Chem. Chem. Phys.*, 2007, **9**, 2531–2537.
57 A. M. Lamsabhi, M. Alcami, O. Mó and M. Yáñez, *ChemPhysChem*, 2003, **4**, 1011–1016.